International Journal of GEOMATE, Aug., 2025 Vol.29, Issue 132, pp.150-157
ISSN: 2186-2982 (P), 2186-2990 (O), Japan, DOI: https://doi.org/10.21660/2025.132.g14386
Geotechnique, Construction Materials and Environment

NON-INVASIVE BASED INFRARED THERMOGRAPHY APPROACH FOR FIELD ASSESSMENT OF SURFACE EROSION IN TAILING DAMS

Vaishnavi Bherde[1], *Umashankar Balunaini[2]

[1, 2] Department of Civil Engineering, Indian Institute of Technology, Hyderabad, India

*Corresponding Author, Received: 08 Dec. 2024, Revised: 08 April 2025, Accepted: 10 April 2025

ABSTRACT: In recent years, non-destructive testing (NDT) has emerged as an efficient tool for evaluating the performance, quality, and integrity of existing structures. This study investigates novel non-destructive techniques, specifically Infrared Thermography (IRT), to detect surface erosion in real-life tailing dams. The tailing dams considered in the study are designed to store coal combustion byproducts in a slurry form, consisting of bottom ash and fly ash. IRT offers a quick and non-invasive monitoring technique to detect, identify, and describe potential anomalies in dykes impacting the integrity of these critical structures. This study captured the thermal images using a FLIR C5 thermal infrared camera during field reconnaissance of an existing starter dyke of a tailing dam located in Northern India. Analysis of these images is facilitated by different software, such as FLIR tools and ResearchIR, enabling the identification of localized temperature variations, which are indicative of potentially affected areas. This study demonstrates the efficiency of IRT in delivering real-time insights into dam conditions, enabling prompt maintenance and action to reduce potential risks. The findings emphasize IRT's ability to monitor and manage dam infrastructure proactively, ultimately improving safety and resilience in tailing management systems.

Keywords: Infrared thermography, Tailing dams, FLIR tools, Erosion detection

1. INTRODUCTION

Tailing dams are a crucial component of infrastructure for many industries, such as the mining industry, power generation, etc. These dams are constructed to collect large amounts of waste products, frequently in the form of slurry that includes ash and other byproducts. According to existing literature, about 1.2% of the 18,000 tailing dams have failed in the past 10 decades. However, the failure rate of conventional water storage dams is 0.01%, pointing out that tailing dams exhibit a significantly higher likelihood of failure [1]. Hence, unlike other dams across the world, the safety and integrity of these tailing dams are also crucial, as breaches can have severe environmental and socioeconomic implications.

Over the past few years, non-destructive testing (NDT) has developed as an important tool for analyzing ground structural response, providing a more efficient and cost-effective approach [2-5]. Several near-surface physical techniques, including ground-penetrating radar (GPR) and optical fiber sensing (OFS), as well as other geophysical techniques like the transient electromagnetic method (TEM) and electric resistivity tomography (ERT), have gained popularity in recent times. The TEM generates a transient electromagnetic field and uses electric currents generated in the subsurface to measure variations in moisture content [6, 7]. However, ERT assesses soil electrical conductivity by examining variations in soil dielectric properties [8, 9]. Other near-surface geophysical methods, such as GPR and OFS techniques, have gained popularity for detecting anomalies. However, they have drawbacks, including high costs, installation challenges associated with laying optical fiber during dam construction, and difficulties with access and monitoring during the flood season [10].

It's worth noting that these NDTs are well-established for field inspection applications, with many other techniques also gaining popularity. Over the past few decades, infrared physics has made tremendous advancements in addressing field-related problems, including the development of handheld and drone-mounted thermal cameras. This progress has established infrared thermography (IRT) as one of the best NDTs available. IRT offers several advantages, such as being a non-contact and non-destructive method, along with providing rapid testing and analysis. Many researchers have utilized this approach for various applications, for example, using portable thermal imagers to locate anomalies in thermal insulation and detect structural issues, highlighting thermography as a valuable non-destructive testing [11]. Furthermore, the feasibility of IRT for identifying defects in the concrete used to stack stone panels, particularly when the panels are thinner than 30 mm, shows its effectiveness for inspecting buildings under specific thermal conditions [12]. Additionally, researchers employed a microbolometer to develop a methodology for quantifying the thermal bridge effect using thermographic surveys and analytical processing [13]. This approach assesses the impact of thermal bridges on overall heat loss in buildings, providing a quantitative assessment factor.

The utilization of the environmental thermographic model (ETM) and remote sensing data from MODIS and Landsat 8 OLI to explore hydrocarbon reservoirs in Lagos, Southern Nigeria, has gained much popularity [14]. By analyzing surface emissivity, temperature, and long-wave radiation, the model effectively identified the potential oil and gas sites, validating their reliability through thermal infrared sources and geological mapping. Additionally, an automatic crack detection system for masonry structures using convolutional neural networks (CNN) to enhance traditional visual inspections. The system integrates CNN with classifiers like support vector machines and random forest (RF), achieving the highest detection accuracy of 86% for the proposed prediction models [15].

Furthermore, researchers studied the 3D model based on an image registration system for change detection in historical structures using unmanned aerial vehicles (UAVs) [16]. By creating 3D models via Structure from Motion (SfM) and synthesizing images with identical camera parameters from the acquired images from UAVs, the system enhances change detection accuracy by minimizing geometrical errors and effectively monitoring damage, such as cracks, over time. The potential of infrared thermography to assess soil properties like porosity and critical state friction angle through cooling rate analysis shows strong correlations ($R^2 > 0.85$) [17]. The method offers a practical approach for in situ soil characterization in geotechnical engineering. Recent studies have explored non-destructive techniques for seepage detection in earthen dams. IRT is a promising method due to its ability to capture thermal anomalies associated with subsurface moisture movement. Laboratory investigations have demonstrated that temperature gradients correlate with seepage rates, offering potential for early detection and integration with drone-based monitoring systems [18].

The next sections of this article go in-depth into the research area and issue statement, highlighting the specific problems of the tailing dam under analysis. The history of Infrared Thermography (IRT) is comprehensively examined, including theoretical concepts and advances in its application. The methodology section describes the approaches, tools, and image-processing processes used in the research. The results and analysis provide the findings of the thermal imaging surveys, emphasizing the observed thermal patterns and their significance. Finally, the conclusion summarizes the important findings, admits limitations, and makes recommendations for future study to enhance non-destructive testing in tailing dam evaluations.

2. RESEARCH SIGNIFICANCE

Although IRT has been used in the past for concrete structures and building inspections, very Few studies have focused on its usefulness in detecting surface erosion in tailing dams. This gap in the literature presents a critical need for further research. With a particular focus on tailing dam applications, this research examines the potential of IRT for identifying surface erosion of the downstream slopes of a tailing dam located in Northern India. These dams store coal combustion byproducts, comprising mainly a mixture of fly ash and bottom ash in the form of water slurry. By utilizing IRT during a field survey of a starter dyke, the research aims to demonstrate IRT's effectiveness in detecting early signs of surface erosion by analyzing thermal data and identifying localized temperature variations. This study seeks to contribute to developing more robust and efficient non-destructive testing (NDT) methods for monitoring the health of tailing dams, ultimately enhancing safety and resilience in tailing management systems.

3. STUDY AREA AND PROBLEM STATEMENT

The Thermal Power Project is located in the Northern part of India. The site includes multiple lagoons: Lagoon-I (for high-concentration slurry deposit), Lagoon-II (a bottom ash lagoon), and Lagoon-III (another bottom ash lagoon). An overflow lagoon connects both Lagoon-II and Lagoon-III, while Lagoon-I is linked to a sedimentation tank (as shown in Fig.1).

Fig.1 Detailed location of six points chosen for the IRT survey

After constructing three functional dykes, surface cracks were observed on the surface of the bund. The extensive deep cuts, longitudinal cracks, and numerous rat holes across the embankment indicate significant structural instability and potential failure risks. Current reports show that these cracks are visible to the naked eye, highlighting the severity of the situation. However, to assess the efficacy of an IRT survey in identifying cracks at early stages, the IRT survey was conducted on the downstream surface at this site. Images were taken at different critical locations to understand the temperature

patterns and thermal color contrast in various scenarios. The results from this study can serve as a benchmark for future IRT-related field studies on dykes. Fig.1 shows the detailed location of six survey points, shown as L1, L2, L3, L4, L5, and L6, where surface cracks are predominantly present.

4. BACKGROUND OF IRT

IRT utilizes electromagnetic radiation emitted by objects with temperatures above absolute zero (-273 °C), falling within the infrared spectrum (wavelengths of 0.75–1000 μm), bridging the gap between microwaves and visible light. IRT is based on several mathematical laws through which temperature measurements are detected by infrared radiation. It is grounded on two major laws. Planck's Law describes how objects emit infrared radiation according to the temperature at which they are maintained, and quantifies the total energy emitted by an object as proportional to the fourth power of its temperature: Stefan-Boltzmann Law. According to thermal radiation theory, a blackbody emits radiation following Planck's law, expressed as:

$$L_\lambda = \frac{C_1}{\lambda^5}\left(e^{\frac{C_2}{T}} - 1\right) \quad \text{Eq (1)}$$

where C_1 and C_2 are constants derived from fundamental physical constants, λ is the wavelength, and T is the temperature. Integrating Planck's law across all frequencies yields Stefan–Boltzmann's law:

$$q_A = \varepsilon\sigma T^4 \quad \text{Eq (2)}$$

where q is the energy emission rate, A is the surface area, T is the absolute temperature, σ is Stefan–Boltzmann's constant, and ϵ is the emissivity (less than unity for real surfaces) [19]. In accordance with Wien's Displacement Law relating temperature to the wavelength (as given in Eq. 3), it is observed that when the temperature of an object increases, the peak wavelength of emitted radiation shifts to shorter wavelengths. For objects at room temperature (around 300 K), the peak emission falls within the infrared range.

$$\lambda_{max} = \frac{b}{T} \quad \text{Eq (3)}$$

where λ_{max} is the peak wavelength, *T* is the temperature in Kelvin, and *b* is Wien's constant (2.897×10^{-3}m·K).

In practice, the emissivity or radiative efficiency of the object, being a material property, significantly influences the temperature measurements. For soils, the emissivity value ranges from 0.90 to 0.95; whereas, grass cover lies between 0.90 and 0.98 [20]. Furthermore, the temperature of an object must be calibrated with the detected emitted infrared radiation (i.e., from the thermal infrared camera). This process involves developing a calibration curve to translate the raw signal into a temperature value. This can be done in two ways: either by measuring known temperature references and developing a mapping between the detected infrared signal and the actual temperature, or by correcting for environmental factors affecting the measurement (viz., atmospheric and reflected temperature and emissivity of the material). In the present study, the second approach is used for the measurements.

Additionally, the radiance data obtained by the infrared camera is converted into temperature using a modified form of Planck's equation (as stated in Eq. (4)). This equation accounts for the camera's response and calibration data. Further, advanced analysis using Fourier transforms is applied to examine thermal patterns over time, which encompasses various applications of thermography, including medical surveys, industrial surveillance, and most recently, in environmental surveillance.

$$T = \frac{C_2}{\ln\left(1+\frac{C_1}{L(\lambda)}\right)\lambda} \quad \text{Eq (4)}$$

where *T* is the temperature of the object in Kelvin, l *(λ)* is the measured radiance at a specific wavelength. C_1 and C_2 are calibration constants that depend on the specific infrared camera and its settings. λ is the wavelength.

IRT techniques are categorized into passive and active methods. Passive IRT captures natural thermal radiation, ideal for detecting temperature differences without external energy. Active IRT uses controlled energy sources like flash lamps or air guns to induce thermal contrast [21]. Both techniques offer distinct advantages: passive for surface-level inspections and active for deeper defect analysis and material property assessments in various sectors, including aerospace, automotive, and building diagnostics.

5. IMAGE PROCESSING

The FLIR C5 infrared thermal camera with an IR resolution of 160 × 120 pixels is used in the present study (as discussed in Table 1). This allows the spatial resolution of the camera to detect enough details to distinguish between objects separated by 6.3 milliradians at a given distance. Further, the FLIR C5 is coupled with an expansive field of view of 54° × 42°, allowing for the capture of expansive scenes without requiring multiple images, which is highly efficient for comprehensive inspections. The temperature measurement range of the camera goes as low as –20°C and as high as 400°C, making it suitable for low-temperature and other high-heat application areas. It can easily detect minute

variations in temperature with a thermal sensitivity of less than 70 mK, which is important for the identification of subtle anomalies in the observed scene. FLIR C5 captures long-wave infrared radiation with a spectral range of 8–14 µm to monitor typical environmental temperatures. This sampling mode involves manual control over the image formation for proper measurement, thus ensuring proper thermal data acquisition with adequate precision for the correct results.

Table 1: FLIR C5 thermal infrared camera specifications

Feature	Value
IR image resolution	160 × 120 pixels
Spatial resolution	6.3 mrad/pixel
Field of view	54° × 42°
Temperature range	–20 to 400°C
Thermal sensitivity	< 70 mK
Spectral range	8–14 µm
Sampling mode	Manual

A critical aspect of IRT analysis involves extracting quantitative temperature data from raw thermal images. In this study, thermal images are enhanced using FLIR Tools and ResearchIR software. Fig. 2 shows the steps involved in thermal image processing. These programs extract unique features from both thermal and optical images, converting them into a fused image through the thermal multi-spectral dynamic imaging (MSX) function. This algorithmic fusion integrates visible spectrum information from the digital camera onto the infrared image, facilitating detailed target alignment.

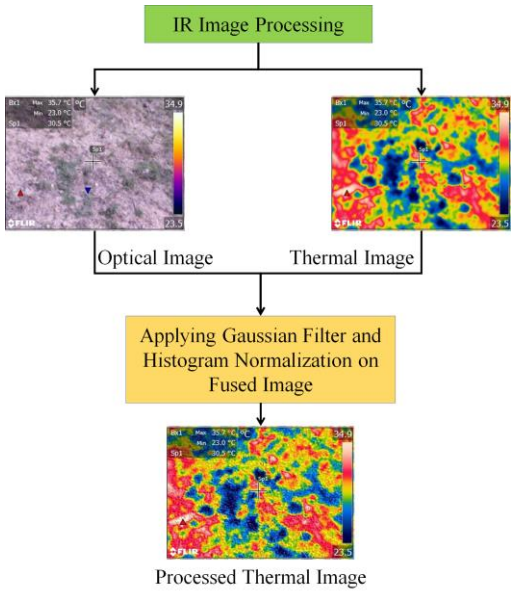

Fig. 2 Steps involved in thermal image processing using FLIR tools

Further processing of the fused image involves applying a Gaussian smoothing filter to reduce background noise, which improves the resolution and makes finer changes more observable during analysis. The histogram of pixel intensities is distributed using histogram equalization, expanding the dynamic range and enhancing the thermal contrast of the image.

6. RESULTS

Accurate thermal images are obtained by providing appropriate input parameters in terms of atmospheric temperature, humidity, and emissivity. While atmospheric temperature and humidity can be measured on-site according to current climatic conditions, emissivity is a surface property with a specific value for different surface types. For soils, the emissivity value ranges from 0.90 to 0.95, whereas grass cover lies between 0.90 to 0.98 [20]. The images were captured on a hot, sunny day on the downstream side of the tailing dam between 10:00 a.m. and 11:30 a.m. Fig. 3 displays the optical images for the various spots selected for the survey. Location 1 (L1) is a plane surface without any rain cuts or undulations. Locations 2 (L2) and 4 (L4) exhibit differential settlement on the slope, with significant rain cuts of approximately 0.3 m deep. At Locations 3 and 5 (L3 and L5), a deep rain cut has formed, measuring about 0.5 meters in depth and width. Additionally, longitudinal microcracks have been observed, continuing from this rain cut. Location 6 (L6) shows damage to the brick lining observed on the kerb portion of the top width of the bund.

Fig. 3 Optical images for different survey locations on the ash dyke

The IR images are processed using the FLIR tool and ResearchIR software. Results are presented using rainbow color contrast with a scale showing the minimum and maximum temperature values, as shown in Fig. 4. In the morning, a temperature difference of approximately 12°C (@ Location 1) is observed on the ground with a generally flat profile. This temperature variation is due to the uneven

heating and cooling rates of the ground surface, influenced by factors such as moisture content, presence or absence of grass turfing, etc. In areas of the ground with deep cuts and large fissures (for example, corresponding to Locations 2, 3, 4, 5, and 6), temperature fluctuations range from 15°C to 29°C.

These areas experience more significant temperature variations because of fractures and cuts, which can create microenvironments where heat is trapped more rapidly than in the surrounding flat areas. During the morning hours, temperatures in locations with deep cuts and significant defects are lower than those of the surrounding profile. Deeper soil, which often has higher moisture content and a more compact structure, tends to have a higher specific heat capacity [22], meaning it requires more heat to raise its temperature compared to the top surface. Additionally, these areas are slower to warm up due to reduced exposure to direct sunlight. As a result, a clear temperature gradient with lower temperatures for the deeper surfaces is observed during peak morning hours.

In the evening, when images are captured for the same locations (as shown in Fig. 5), the temperature gradient becomes more uniform, reducing to nearly 5°C. This is because the deeper soil, with a higher specific heat capacity, can store more heat during the day but also loses heat more quickly once the external heat source (sunlight) is removed. The heat stored in the soil is lost to the cooler evening and night air through the surface. The soil emits infrared radiation throughout the night, decreasing its overall temperature. The hot spots on deeper surfaces for particular imaging frames remain more pronounced than the plane ground.

Figure 6 presents temperature differences ($T_{max} - T_{min}$) recorded at various locations with different defect depths using a thermal infrared camera, highlighting the thermal bridge effect (a phenomenon where deeper defects cause greater temperature variations due to disrupted heat flow). Depth values were obtained through direct on-site measurements using a calibrated scale, not inferred from thermal imagery. The IR images, captured at a resolution of 160 × 120 pixels, visually correlate to defect depth with temperature variation but do not serve as a depth estimation method. The images are captured from a 2-meter distance, covering approximately 3.14 m² (2.04 m × 1.54 m) based on the field of view (FoV) of the camera (equal to 54° in horizontal and 42° in vertical), ensuring sufficient spatial resolution for defect analysis.

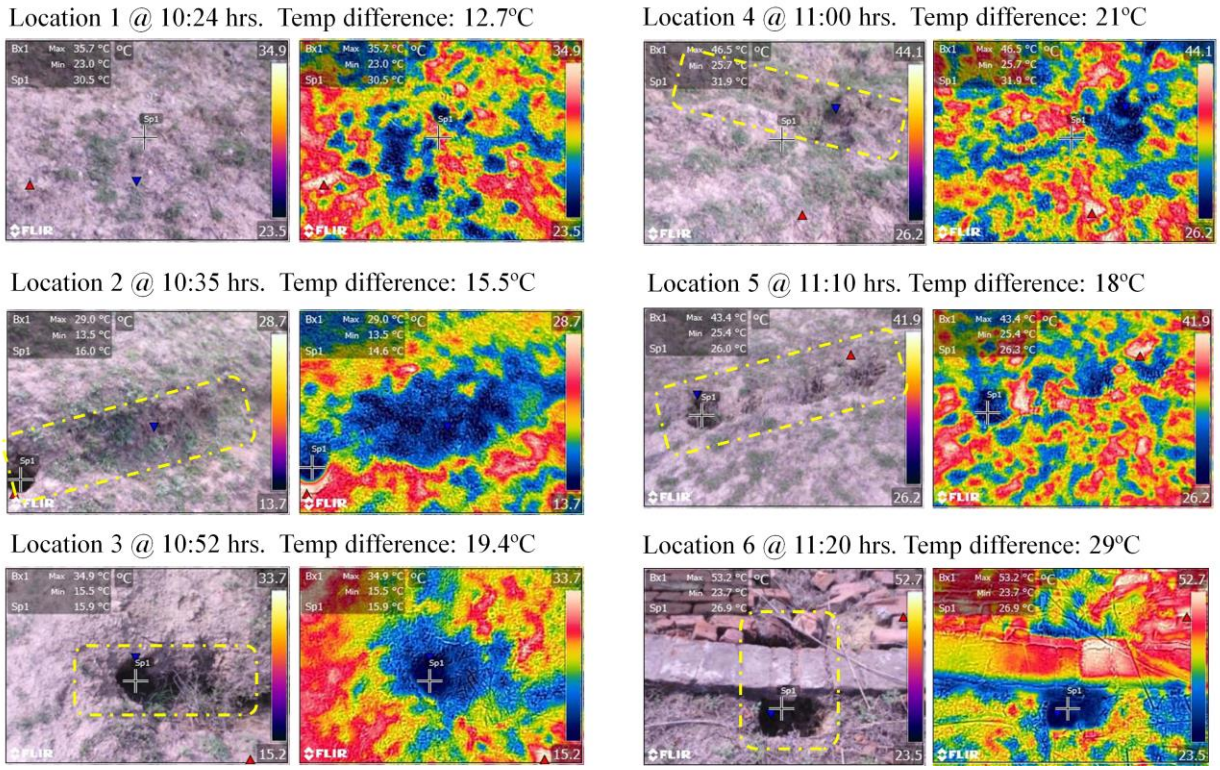

Fig. 4 Optical and corresponding IR Images captured from FLIR C5 thermal infrared camera for different locations during morning hrs. (defects are highlighted yellow in the optical image in the photos)

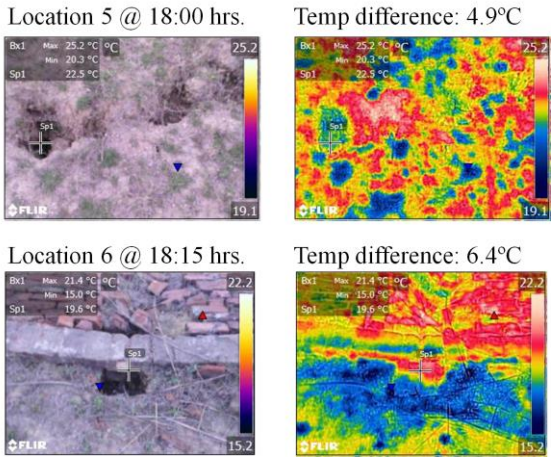

Fig. 5 Optical and corresponding IR Images captured from FLIR C5 thermal infrared camera for different locations during evening hrs.

The infrared camera detects temperature variations around the cracks due to the relative difference in specific heat capacity between the surface and deeper soil within the embankment, which disrupts natural heat transfer. This differential thermal behavior highlights the cracks and deep cuts. In the morning, when the embankment is cooler, the reduced heat flux towards the surface due to the presence of cracks results in a localized cooler zone, appearing blue in the IR image. This creates a higher temperature difference between the defect area and the surrounding profile. Conversely, in the evening, when the embankment has warmed up, the increased heat transfer through the crack creates a localized warmer zone, appearing as a hot spot in the IR image, leading to a lower temperature difference between the defect area and the surrounding profile.

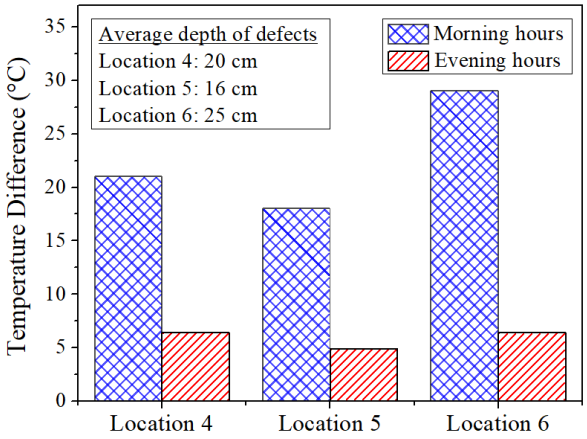

Fig. 6 Temperature variation at different locations

Fig. 7 depicts the relationship between the average depth of erosion and temperature difference derived from thermal infrared (IR) images captured during morning hours. The temperature difference ($T_{max} - T_{min}$) is obtained from the thermal color contrast of IR images at different locations (L1–L6). The results demonstrate an increasing trend, signifying that deeper erosion sites exhibit higher temperature differentials due to the thermal bridge effect, indicating greater heat retention and dissipation variations.

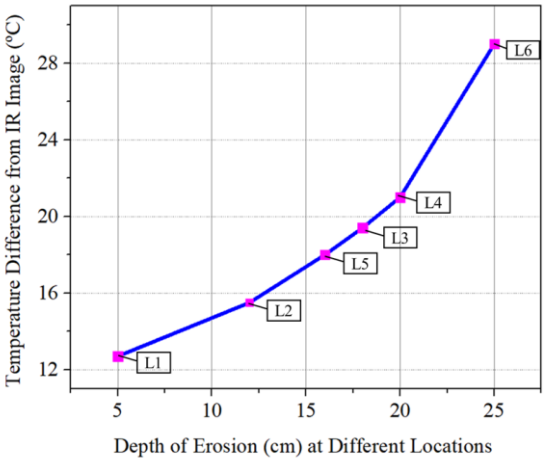

Fig. 7 Correlation between temperature difference and depth corresponding to morning hours

The IR camera takes advantage of this contrast in thermal conductivity to visualize cracks, even those invisible to the naked eye. This allows for the proactive identification of potential weaknesses in the embankment before they escalate into critical issues. The size and depth of the crack influence the magnitude of the temperature variation, with larger cracks creating more pronounced anomalies. Additionally, stable ambient temperatures during inspections are preferred to minimize misinterpretations caused by rapid temperature fluctuations. In summary, IR cameras effectively detect cracks in earthen embankments by exploiting the differing thermal properties of soil and air, aiding in maintaining structural integrity.

7. CONCLUSIONS

Tailing dams are essential to many sectors, but their structural integrity is essential considering environmental safety. Although there are many conventional approaches to checking the structural integrity of these dams. However, the present study investigates the application of IRT as a non-destructive testing method for identifying surface erosion in tailing dams. The research focused on the starter dyke at a site known to have extensive surface cracks and deep cuts. Field surveys were conducted at six critical locations, and the results were promising. IRT successfully identified these areas of concern based on the thermal variations it detected.

During the day, the areas with cracks exhibited temperature variations ranging from 15°C to 29°C, a clear deviation from the surrounding regions. The study concluded that this difference in temperature

profile depends on the size of holes, cracks, differential heaving, and other anomalies present on the surface. The temperature response of cracked areas was also found to differ depending on the time of day, for instance, the reduction in temperature for Location 6 is observed from 29°C to 6°C. During the morning, the temperature contrast between cracked and non-cracked areas was more noticeable compared to the evening. This phenomenon occurs due to reduced solar radiation during the evening or nighttime, causing defective areas to lose heat faster overnight and warm up slower in the morning. Conversely, during the evening, these defects facilitate rapid heat transfer, resulting in higher temperatures in these areas.

Overall, IRT can serve as a useful tool for monitoring temperature differences; however, it has several limitations that may restrict its usefulness and wider implementation. Its dependency on weather conditions is a major drawback; extreme temperature fluctuations and rainfall can misinterpret the thermal imaging patterns. Furthermore, surface moisture can tamper with the thermal signatures of the cracks, making it difficult to examine the underlying problems with full accuracy. In addition, the results may be misinterpreted due to the limited resolution of infrared cameras. However, some highly sophisticated models can capture minute temperature variations, leading to more comprehensive results. Additionally, further research is needed to explore IRT's ability to measure crack depth and to track its development over time. Finally, combining IRT data with other NDT techniques, such as ground-penetrating radar or electrical resistivity tomography, could enhance the assessment of dam integrity.

8. ACKNOWLEDGMENTS

This work is supported by the Department of Science and Technology (DST) National Mission on Interdisciplinary Cyber-Physical Systems (NM-ICPS), Technology Innovation Hub on Autonomous Navigation and Data Acquisition Systems: TiHAN Foundations at Indian Institute of Technology (IIT) Hyderabad.

9. REFERENCES

[1] Lyu Z., Chai J., Xu Z., Qin Y., Cao J., A comprehensive review on reasons for tailing dam failures based on case history. Advances in Civil Engineering, Vol 2019, Issue 1, 2019, pp.1–18.

[2] Rens K.L., Wipf T. J., Klaiber F. W., Review of nondestructive evaluation techniques of civil infrastructure. Journal of Performance of Constructed Facilities, Vol 13, Issue 1, 1997, pp. 47-48.

[3] Shabani F., Asadizadeh M., Hedayat A., Tunstall L., Gorman B. P., Gonzalez, J. A. V., Alvarado J. W. V., and Neira M. T., Evaluation of Fracture Properties in Ceramics Made of Sulfidic Mine Tailings. Rock Mechanics and Rock Engineering, 2024, pp.1-19.

[4] Chen Q., and Zhongjie Z. Feasibility Study on Use of Drone-Based Infrared Thermography for Soil Moisture Detection in Highway Embankment and Dam Inspections. Journal of Infrastructure Systems 31, no. 1, 2025, pp. 04024033.

[5] Zhang Z., and Qiming C. Exploration of Drone and Remote Sensing Technologies in Highway Embankment Monitoring and Management (Phase I). No. FHWA/LA. 23/690. 2023.

[6] Nabighian M.N., and Macnae J., Time domain electromagnetic prospecting methods. In Society of Exploration Geophysicists eBooks, 1991, pp. 427–520.

[7] Wang Y., Jia Y., Liang J., Tang L., Guan F., Li P., Zhang S., and Tian H., Crack depth measurement and key points of accurate identification in concrete structures: a review. Nondestructive Testing and Evaluation, 2024, pp.1-35.

[8] Cardarelli E., Cercato M., and De Donno G., Characterization of an earth-filled dam through the combined use of electrical resistivity tomography, P-and SH-wave seismic tomography and surface wave data. Journal of Applied Geophysics, Vol 106, 2014, pp. 87-95.

[9] Franco L. M., La Terra E. F., Panetto L. P., & Fontes S. L., Integrated application of geophysical methods in Earth dam monitoring. Bulletin of Engineering Geology and the Environment, Vol 83, Issue 2, 2024, pp. 62.

[10] Daniels D. J., Gunton D. J., & Scott H. F., Introduction to subsurface radar. In IEE Proceedings F (Communications, Radar and Signal Processing), Vol. 135, Issue 4, 1988, pp. 278-320

[11] Titman D. J., Applications of thermography in non-destructive testing of structures. NDT & e International, Vol 34, Issue 2, 2001, pp. 149-154.

[12] Cerdeira F., Vázquez M. E., Collazo J., and Granada E., Applicability of infrared thermography to the study of the behavior of stone panels as building envelopes. Energy and Buildings, Vol 43, Issue 8, 2011, pp. 1845-1851.

[13] Asdrubali F., Baldinelli G., & Bianchi F., A quantitative methodology to evaluate thermal bridges in buildings. Applied Energy, Vol 97, 2012, pp. 365-373

[14] Emetere M. E., Samuel E. S., Jennifer M. E., and Uno E. U. Thermal infrared remote sensing of hydrocarbon in Lagos-Southern Nigeria: Application of the thermographic

model. International Geomate Journal 13, no. 39, 2017, pp. 33-45.
[15] Chaiyasarn K., Mayank S., Luqman A., Wasif K., and Nakhon P. Crack detection in historical structures based on convolutional neural network. GEOMATE Journal 15, no. 51, 2018, pp. 240-251.
[16] Buatik A., Luqman A., and Krisada C. 3D model-based image registration for change detection in historical structures via unmanned aerial vehicle. GEOMATE Journal 16, no. 58, 2019, pp. 132-138.
[17] Loche M., Gianvito S., Jan B., and Filip H. Investigating the Potential of Infrared Thermography to Inform on Physical and Mechanical Properties of Soils for Geotechnical Engineering. Remote Sensing 14, no. 16, 2022, pp. 4067.
[18] Bherde V, Balunaini U. Laboratory investigations on infrared thermography-based seepage detection in earthen dams. *In: Geotechnical Frontiers 2025*, pp. 38–45.
[19] Bagavathiappan S., Lahiri B. B., Saravanan T., Philip J., and Jayakumar T. Infrared thermography for condition monitoring–A review. Infrared Physics & Technology, Vol 60, 2013, pp. 35-55.
[20] French A. N., Schmugge T. J., and Kustas W. P. Discrimination of senescent vegetation using thermal emissivity contrast. Remote Sensing of Environment, Vol 74, Issue 2, 2000, pp. 249-254.
[21] Balaras C. A., and Argiriou A. A., Infrared thermography for building diagnostics. Energy and buildings, Vol 34, Issue 2, 2002, pp. 171-183.
[22] Nofziger D. L. Soil temperature changes with time and depth: theory. /http:// soilphysics.okstate.edu/software/SoilTemperature/document.pdfS.